DESIGN OF A DROP IMPACT TEST RIG FOR ACCELEROMETER VALIDATION FOR TURBOCHARGER APPLICATION

Article history
Received
8th September 2021
Revised
1st January 2022
Accepted
12th June 2022
Published
22nd June 2022

Mahadhir Mohammad[1], Meng Soon Chiong[1,2,*] Mohd Aizuddin Nyan[2], Muhammad Hanafi Md Sah[1] and Malarvili Balakrishnan[3]

[1] UTM LoCARtic
Universiti Teknologi Malaysia, 81310 UTM Johor Bahru, Johor, Malaysia

[2] School of Mechanical Engineering, Faculty of Engineering
Universiti Teknologi Malaysia, 81310 UTM Johor Bahru, Johor, Malaysia

[3] School of Biomedical and Health Science Engineering,
Faculty of Engineering
Universiti Teknologi Malaysia, 81310 UTM Johor Bahru, Johor, Malaysia

[*]Corresponding email: chiongms@utm.my

ABSTRACT

Automotive turbochargers increase internal combustion engine power and efficiency in passenger and commercial vehicles. The vibrational characteristics need to be closely monitored during testing as it indicates the state of the turbocharger and its components. For this purpose, an accurate accelerometer is a must. This paper presents the design of a drop impact test rig for accelerometer validation. The design is based on ASTM E1876 standard and able to cover a frequency range of 0-6000 Hz. This represents a typical turbocharger operating speed of up to 120,000 rpm, with four common types of vibrational mode expected – synchronous, sub-synchronous, harmonic, and non-synchronous. Three materials have been selected for the specimen plate, namely ABS, Copper and AISI 1050 steel. The abovementioned frequency range can be satisfied by varying the specimen thickness. The drop impact test rig allows four different drop heights. Further combined with four different steel ball sizes, the magnitude of induced acceleration can be manipulated during the drop test. This drop impact test rig enables on-site accelerometer validation before any turbocharger gas stands testing, which is crucial for an accurate vibrational measurement.

Keywords: *Turbocharger, Vibration analysis, High speed machine, Experimental Testing, Rotordynamics*

1.0 INTRODUCTION

A turbocharger is a special class of turbomachinery intended to improve the efficiency of internal combustion engines in passenger and commercial vehicles by utilizing the waste energy in the exhaust gases. Nowadays, a turbocharged engine is becoming a standard practice in the automotive industry to acquire a higher power-to-weight ratio and better fuel economy. This is realized via engine downsizing, whilst maintaining the equivalent engine output by increasing the engine inlet air density.

However, according to Watson and Janota [1], turbomachines such as turbines can only operate effectively at a small operating range that is highly dependent on the incidence flow

angle at the inlet of the rotor. Any rotating machinery may experience vibrations, including turbochargers. The measurement of a periodic oscillation process with respect to an equilibrium point is known as mechanical vibration. There can be four types of mechanical vibration, namely the sub-synchronous, synchronous, non-synchronous and harmonic to prolong the lifetime and efficiency of a turbomachine, it is important to monitor the amplitude of these vibrations during operation.

An industrial device is designed to run quietly and without vibration. Any vibration indicates problems in these machines or equipment deterioration. Machine vibration that is left unchecked can hasten the wear and damage. Vibrating machinery also produces excessive noise, pose a safety hazard, and degrading the plant working conditions [2]. Vibration leads to the deterioration of machinery's efficiency, consuming more energy and resulting in poor product quality. In the worst-case scenario, vibration can severely damage equipment, forcing it out of service and halting plant production.

The vibrational analysis can be measured using a piezoelectric accelerometer. The piezoelectric crystal generates an electrical charge in response to the acceleration (vibration) when the accelerometer is installed on the machine. The calibration and validation of the accelerometer are important to ensure the measurement is accurate. In this paper, a test rig for accelerometer validation has been designed. The validation rig is capable to emulate vibration of various frequencies and amplitudes typically found in automotive turbochargers. Thereby, an accelerometer can be check for accuracy before the start of any experiment. The test rig is designed based on theoretical calculation of vibration and the expected result is presented in this paper.

1.2 Turbocharger Vibration

Synchronous vibration occurs at the rotating shaft speed of 1X RPM. There are five sources of synchronous vibration which is unbalance, eccentricity, mechanical looseness, overhung unbalance and resonance. Sub-synchronous vibration occurs at less than the shaft turning speed (less than 1X RPM). For this type of vibration, there are three primary sources found in a turbocharger which is oil whirl, oil whip and journal bearing. The harmonic vibration occurs due to bent shaft and looseness in the system. Harmonic vibration is always a multiply of the operation speed, i.e., 1X, 2X … *n*X RPM in the system. Lastly, non-synchronous vibration is not equal to the multiply of shaft speed. It can be less than 1X RPM or not equal to any *n*X RPM. Non-synchronous vibration occurs due to aerodynamic problems during these four situations: non-uniformly flow in the inlet and outlet, operating in flutter region of compressor map, rotating stall and at compressor surge operation.

1.3 Turbocharger Cold Flow Mapping

For cold flow gas stand turbocharger in UTM LoCARtic, the turbocharger operated at four different speeds: 60, 90, 105 and 120kRPM. At each speed, multiple points represent different operating conditions of a turbocharger will be tested. As seen in the compressor map in Figure 1, the first point of every speed line starts near the choke condition, while the last point ends at the surge condition. Table 1 shows the corresponding range of operating frequency from the operating condition in Figure 1.

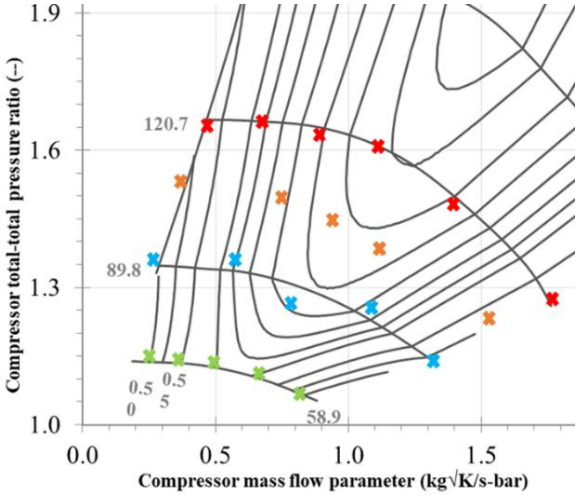

Figure 1 Turbocharger operating points on LoCARtic turbocharger gas stand

Table 1 Range of turbocharger operating frequency on LoCARtic turbocharger gas stand

RPM	0.25X	0.5X	0.7X	1X	2X	3X
60,000	250	500	700	1000	2000	3000
90,000	375	750	1050	1500	3000	4500
105,000	437.5	875	1225	1750	3500	5250
120,000	500	1000	1400	2000	4000	6000

2.0 METHODOLOGY

There are four methods to validate the measurement of an accelerometer, namely the shock hammer test, back-to-back accelerometer, inversion test and drop impact test. The shock hammer test and back-to-back accelerometer test utilize a modal hammer [3] and shaker [4] as an impulser to induce known vibration to a specimen where the accelerometer is attached to. These two methods are highly dependent on the accuracy of the reference (pre-calibrated) accelerometer hence not sustainable for the current application. On the contrary, an inversion test and drop impact test rely on the gravitational acceleration thus insensitive to any pre-calibrated instrumentation, making it a more robust solution.

During an inversion test, when the accelerometer is positioned upright as shown in Figure 2a, the gravitational acceleration imposed to the accelerometer is -9.81 m/s2 or -1 g. When the accelerometer is inverted upside down as shown in Figure2b, the subjected acceleration would be +9.81 or +1g. For the same principle, the accelerometer will measure 0 g with no acceleration when placed horizontally. The downside of an inversion test is that it can only achieve 3 validation points between ±1 g [5]. This may not cover most real-life applications.

On the other hand, a drop impact test works by dropping an object onto a horizontal (specimen) surface. The object begins at rest position and free-falls to affect a rigid surface after moving a distance, *h*, as shown in Figure 3. The object then bounces upwards to a height of *d* after impact. A lighter object will tend to exhibit shorter pulse width and include vibration with greater amplitude when dropped from the same height and vice versa [6]. The vibrational frequency is dependent on the material and dimension of the specimen on which the object is falling onto. Therefore, by varying the dropping height, falling object mass, specimen material and dimension, the frequency and amplitude of induced vibration may be varied according to the desired range.

The drop impact test requires the knowledge of material's elastic properties. This can be identified via a destructive or non-destructive method. The impulsive excitation technique, also known as a dynamic mechanical test, is one of the non-destructive methods.

It involves setting a sample into mechanical vibration in one or more vibrational modes at one or more frequencies where the vibrational displacements are at their maximum.

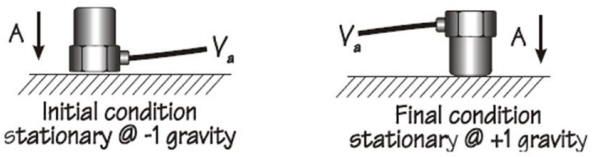

(a) (b)

Figure 2 Inversion test diagram: (a) upright position (b) upside down position [5]

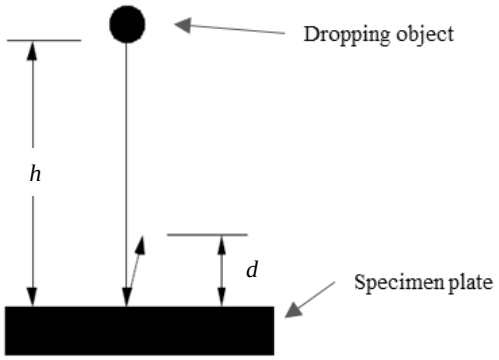

Figure 3 Drop impact test diagram [6]

The elastic properties of the material can then be determined by knowing the vibrational modes, the natural frequencies of the vibration decay, the mass and dimension of the specimen plate [7]. Through the impulsive excitation technique, a drop impact test can be conducted without the need to perform a separate test to determine the elastic properties of the specimen plate. Instead, it can be computed via the methodology to be presented in Section 3.0 while calculating the induced acceleration [4].

There are seven criteria to be fulfilled in selecting an accelerometer which is amplitude, sensitivity, number of axes, the weight of accelerometer, mounting option and environmental constraints [8]. The accelerometer to be used in this drop impact test rig is a lightweight (2.0 gm) stud-mount Quartz unit. It is capable of measuring between the range of ±500 g pk with a sensitivity of 10 mV/g, and from 1.0 to 10,000 Hz with ±5% of accuracy. Its lightweight construction ensured the vibration experienced by the accelerometer is always in-synchronous with the machine – without inertia effect, while stud mount ensured the vibration amplitude is not dampened out during measurement.

3.0 MATHEMATICAL MODELING

Theoretical calculation plays an important role in this drop impact test rig design. It predicts the initial result of the drop impact test, which in turn, help set the design parameter of the rig and material selection for the specimen plate. At the same time, the result also serves as the reference value for an accelerometer to be validated with. Four common materials for the specimen plate of a drop impact test rig are chosen for the analysis here. Their mechanical properties are given in Table 2 [9]. The methodology for computing their elastic properties and the resultant vibrational acceleration from the drop impact test will be presented in this section.

From Table 1, it was found that the operating frequency of a turbocharger on the UTM LoCARtic gas stand is ranging from 0 to 6000 Hz, corresponds to 60,000 to 120,000 RPM

turbocharger speed. By knowing the range of frequency spectrum, further analysis has been done.

Table 2 Mechanical properties of different specimen plate materials for drop impact test [9]

Material	Young Modulus (GPa)	Poison Ratio	Density (kg/m^3)	Shear Modulus (GPa)
AISI 1050 Steel	200	0.29	7870	80
Acrylonitrile Butadiene Styrene (ABS)	2.07	0.394	1050	2.02
Copper, Cu; Annealed	110	0.343	8930	46
Aluminium 1100-H14	68.9	0.33	2710	26

For a simply supported plate, the shape function *W* is taken as

$$\boldsymbol{W(x,y) = \sum_{m=1}^{\infty}\sum_{n=1}^{\infty} C_{mn}\frac{m\pi x}{a}\sin\frac{n\pi y}{b}} \quad (1)$$

where *a*, *b* and *t* are the length, width and thickness of the specimen plate and C_{mn} is the vibration amplitude for each value of *m* and *n* – the mode number in each direction. The specimen plate's natural frequency, ω_{mn} can then be expressed as:

$$\boldsymbol{\omega_{mn} = \sqrt{\frac{D}{\rho t}}\left[\left(\frac{m\pi}{a}\right)^2 + \left(\frac{n\pi}{b}\right)^2\right]} \quad (2)$$

where ρ is the density of the plate. The elastic property of the specimen plate expressed in the Flexural Rigidity, *D* is given as

$$\boldsymbol{D = \frac{Et^3}{12(1-\vartheta^3)}} \quad (3)$$

where *E* is Modulus of Elasticity and ϑ is Poisson's Ratio of the material. Kirchhoff-Love plate theory is considered valid since the aspect ratio of the specimen plate, $t/b \ll 0.1$ in all cases. From the natural frequency obtain in equation 2, the induced frequency, *f* in Hertz is calculated using equation 4 below.

$$\boldsymbol{f = \frac{\omega_{mn}}{2\pi}} \quad (4)$$

Based on the law of conservation of energy, the potential energy, *PE* before the event must equal to kinetic energy, *KE* after the event. It then translates into potential energy representable as a spring system, PE_{Spring} given by equation 7 For the simple drop impact test, *m* = mass, *h* = drop height, *g* = gravitational acceleration, *v* = impact velocity, *k* = spring rate and *d* = the spring displacement.

$$\boldsymbol{PE = mgh} \quad (5)$$

$$\boldsymbol{KE = \frac{1}{2}mv^2} \quad (6)$$

$$\boldsymbol{PE_{Spring} = \frac{1}{2}kd^2} \quad (7)$$

The displacement, *d*, would be a combination of the deflection of both the falling components and the impact surface and the spring rate, *k*, is a combination of the component stiffness and the stiffness of the impact surface. Since energy must be conserved, the potential energy prior to the drop, *PE*, must be equal to the kinetic energy immediately prior to impact, *KE*, which in turn must be equal to the maximum energy stored in the spring system when the velocity is zero at the maximum impact depth, PE_{Spring}. Thus:

$$\boldsymbol{mgh = \frac{1}{2}mv^2 + \frac{1}{2}kd^2} \quad (8)$$

Rearranging and solving for d when $v = 0$, gives:

$$\boldsymbol{d = \sqrt{\frac{2mgh}{k}} = \sqrt{2gh}\sqrt{\frac{m}{k}} = \frac{\sqrt{2g}}{\omega}\sqrt{h}} \quad (9)$$

Equation 9 makes the substitution for the system natural frequency, ω and shows that the impact depth, d is a function of frequency and the square root of the drop height, h. For greater impact depths, the impact time will of necessity be proportionately longer. Displacement is naturally given as a function of acceleration and impact velocity by the well-known relation:

$$\boldsymbol{d = d_0 + v_0 t + \frac{1}{2}AT^2} \quad (10)$$

For a traditional haversine shock, the velocity, v change is a function of the pulse width duration, T and the maximum acceleration, A as:

$$\boldsymbol{v_0 = \frac{1}{2}AT} \quad (11)$$

Substituting equation 11 into equation 10 and making the initial condition $d_0 = 0$ yields:

$$\boldsymbol{d = AT^2} \quad (12)$$

Thus, the impact time, T is proportional to the square root of impact depth, d, at the same time, the fourth-root of the drop height, h (from equation 9). The peak acceleration in a drop shock is dependent on the inverse pulse width. The shorter pulse width result higher accelerations. The final acceleration in a drop shock is defined in equation 13, where it is a function of square root to drop height, h and the impact depth (rebound distance) d; and g is the gravity and T pulse width or impact time.

$$\boldsymbol{A = \frac{\pi}{T}\sqrt{\frac{g}{2}}(\sqrt{h + d})} \quad (13)$$

4.0 RESULTS AND DISCUSSION

Figure 4 shows the drop impact test rig and its constituent components. The design is based on the ASTM E1876 standard [10]. It allows four different drop heights, from 0.5m to 2.0m, in a 0.5m increment. The accelerometer is positioned 13.3 cm from the centre of the rectangular specimen plate.

The specimen plate is simply supported at 0.224a from each end for a flexural mode of vibration. The triangular supports are made of steel, providing simple support to the specimen with minimal restriction to the resultant vibration during the drop test. Two temporary guides shall be used to position the specimen plate before every drop impact test for consistent placement. This ensures that the ball hits the centre of the specimen consistently – crucial for a precise accelerometer reading during the verification test. Steel ball (with a diameter ranging from 12.5 mm to 50.8 mm) was held at its initial position by a 12VDC electromagnet. The vibration response of the specimen plate is measured and recorded by the accelerometer. Recorded signals can then be converted to the frequency domain using the Fast Fourier Transform (FFT) algorithm to obtain the frequency peak values.

Table 3 shows the flexural rigidity for four specimen materials of five thicknesses. The length and width of these specimens are maintained at 400mm x 250mm (a x b). By using Equations 3–5, the natural frequency of these combinations can be determined. The thickness of these materials is varied to achieve different natural frequencies. The corresponding natural frequencies for AISI 1050, ABS, Copper and Aluminum 1100-H14

are tabulated in Tables 4–7 respectively. The results from Table 4–7 is also plotted into the spectrum range in Figure 5 from 0Hz to 6000 Hz – covering the expected vibrational frequency as stated in Table 1.

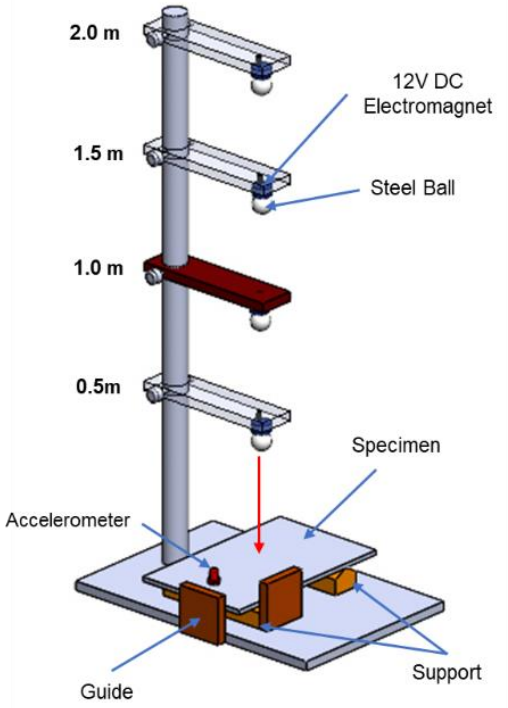

Figure 4 Final design of the drop impact test rig for accelerometer measurement validation

Table 3 Flexural Rigidity of different material and thickness, *t* (mm) combination

Material \ Thickness, *t* (mm)	1	5	10	15	20
	Flexural rigidity, D (Nm^2)				
AISI 1050	18.2	2274.6	18197.0	61415.0	
ABS		25.5	204.2	689.2	1633.6
Copper		1298.6	10388.9	35062.6	
Aluminium 1100-H14		805.4	6443.3	21746.3	51546.8

Table 4 Natural frequency of different AISI 1050 specimen thickness, *t* (mm)

Thickness, *t* (mm)	Frequency, *f* (Hz)			
	f_1	f_2	f_3	f_4
1	53.14	167.79	358.88	626.40
5	265.73	838.97	1794.39	3131.98
10	531.45	1677.95	3588.78	6263.95
15	797.18	2516.93	5383.17	9395.93

Table 5 Natural frequency (Hz) of different ABS specimen thickness, *t* (mm)

Thickness, *t* (mm)	Frequency, *f* (Hz)			
	f_1	f_2	f_3	f_4
5	77.06	243.31	520.4	908.31
10	154.13	486.62	1040.79	1816.63
15	231.19	729.94	1561.18	2724.95
20	308.26	973.26	2081.60	3633.27

Table 6 Natural frequency (Hz) of different copper specimen thickness, *t* (mm)

Thickness, *t* (mm)	Frequency, *f* (Hz)			
	f_1	f_2	f_3	f_4

5	188.49	595.11	1272.81	2221.59
10	376.97	1190.21	2545.62	4443.19
15	565.46	1785.32	3818.43	6664.78

Table 7 Natural frequency (Hz) of different Aluminium 1100-H14 specimen thickness, *t* (mm)

Thickness, *t*	**Frequency, *f* (Hz)**			
(mm)	f_1	f_2	f_3	f_4
5	269.46	850.76	1819.60	3175.97
10	538.92	1701.52	3639.20	6351.94
15	808.37	2552.28	5458.79	9527.91
20	1077.83	3403.04	7278.39	12703.88

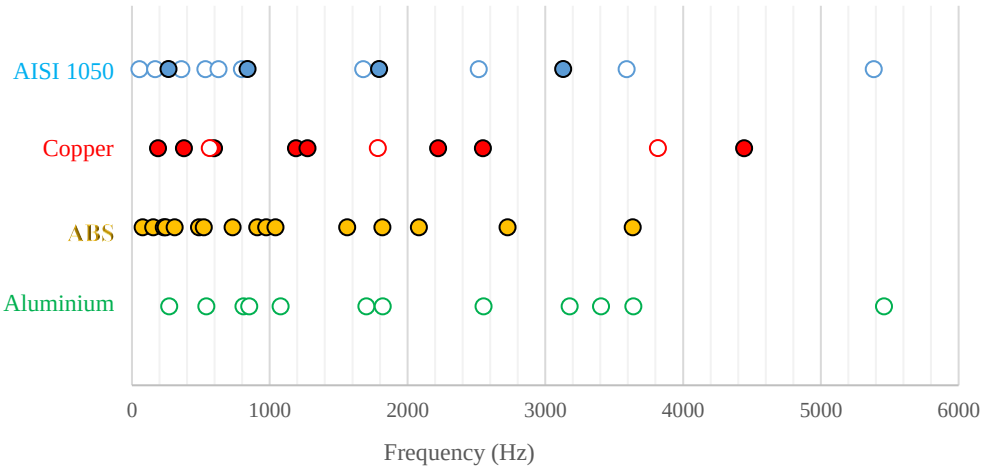

Figure 5 Natural frequency of different specimen material and thickness (filled markers indicates the chosen specimen material to be used for the drop impact test rig).

From the height of the impact, the resultant velocity and impact force can be calculated using Equations 9 and 13. The results are provided in Tables 8 and 9. A lighter object will exhibit shorter pulse widths, *T* and greater acceleration when dropping from the same height, *h*. On the other hand, a heavier object will impart greater force to the specimen but with lower acceleration [11].

Table 8 Impact velocity, *v* (m/s) with respect to drop height, *h* (m)

Drop height, *h* (m)	**Impact velocity, *v* (m/s)**
0.5	3.13
1.0	4.43
1.5	5.42
2.0	6.26

Table 9 Impact force (N) of ball size with respect to drop height, *h (m)*

Steel ball	**Mass, *m***	**Drop height, *h* (m)**			
diameter (mm)	**(kg)**	0.5	1.0	1.5	2.0
12.7	0.00843	0.042	0.083	0.124	0.170
25.4	0.0674	0.330	0.661	0.990	1.320
38.1	0.228	1.120	2.240	3.350	4.470
50.8	0.54	2.650	5.300	7.930	10.580

From the results in Tables 3–9 and Figure 5, the chosen material and thickness for the specimen plate are summarized in Table 10. First, ABS material of 4 different thicknesses from 5mm to 20mm are selected to cover the frequency range, as shown by the filled markers in Figure 5. Next, copper material of 5mm and 10mm, and AISI 1050 of 5mm

thickness will be used to cover the frequency gap of ABS material. Four steel ball sizes will be used during accelerometer validation, along with four drop heights to achieve different combinations of acceleration magnitude.

Table 10 Dimension of specimen used for drop impact test and its corresponding induced frequency, *f* (Hz)

Material	Specimen plate dimension (mm)			Induced frequency, *f* (Hz)
	Length, *a*	Width, *b*	Thickness, *t*	
ABS	400	250	5	77.06 - 908.31
ABS	400	250	10	154.13 - 1816.13
ABS	400	250	15	231.19 - 2724.95
ABS	400	250	20	308.26 - 3633.27
Copper	400	250	5	188.49 - 2221.59
Copper	400	250	10	376.97 - 4443.19
AISI 1050	400	250	5	265.73 - 3131.98

5.0 CONCLUSION

In conclusion, an accelerometer validation rig for turbocharger application has been designed in this paper. The drop impact test rig is capable of covering the entire range of typical turbocharger operation on a gas stand testing. Three types of materials have been selected for the specimen plate to cover the frequency range of 0 to 6000Hz. All specimen plates, regardless of material, have a fixed length and width but varying in thickness. The expected result can be calculated using theoretical formulae demonstrated in this paper during accelerometer validation.

ACKNOWLEDGMENT

The author would like to acknowledge the Ministry of Higher Education Malaysia (MoHE) for funding of this research – under registered program cost centre: #R.J130000.7851. 5F111.

NOMENCLATURE

A	Acceleration	k	Spring rate
a	Length of specimen	m	Mass / mode number of vibration
ABS	Acrylonitrile Butadiene Styrene	n	Mode number of vibration
b	Width of specimen	PE	Potential energy
C	Vibration amplitude	RPM	Revolution per minute
D	Flexural rigidity	T	Time
d	Bounce or impact height or spring displacement	t	Thickness of specimen
d_0	Initial bounce or impact height	v	Velocity
FFT	Fast Fourier Transform	W	Shape function
f	Frequency		
g	Gravitational acceleration	ρ	Density
h	Drop height	ϑ	Material Poisson's ratio
KE	Kinetic energy	ω	Natural frequency

REFERENCES

1. Watson N, Janota MS. *Turbocharging the internal combustion engine*. The Macmillan Press Ltd.; 1982.
2. Holmes, R., 2002. Turbocharger Vibration - A Case Study. *IMechE Conference Transactions C692/031/2002. Seventh International Conference on Turbochargers and Turbocharging.*
3. Sanliturk KY and Koruk H (2013). Development and validation of a composite finite element with damping capability. *Composite Structures*, 97: 136-146.
4. Accelerometer Calibration Using the VR9500 Tutorial - Vibration Research. Vibration Research. (2021). Available online at https://vibrationresearch.com/resources/ accelerometer-calibration-using-the-vr9500/. [Assessed: 31 July 2021]
5. Modalshop.com. (2021). *Basic of Calibration*. Available online at http://modalshop.com/filelibrary/Basics%20of%20Calibration.pdf. [Accessed: 30 July 2021]
6. Endevco.com. (2021). *Acceleration level of drop test*. Available online at https://endevco.com/contentStore/mktgContent/endevco/dlm_uploads/2019/02/TP321.pdf. [Accessed: 30 July 2021]
7. Botelho EC, Campos AN, De Barros E, Pardini LC, and Rezende MC, 2006. Damping behavior of continuous fiber/metal composite materials by the free vibration method. *Composites Part B: Engineering*, 37(2): 255-263.
8. National Instrument (2021). Measuring Vibration with Accelerometers. Available online at https://www.ni.com/en-my/innovations/white-papers/06/measuring-vibration-with-accelerometers.html. [Accessed: 26 January 2021]
9. MatWeb (2021). Material property data. Available online at http://www.matweb.com/. [Assessed: 29 November 2021].
10. ASTM (2015). ASTM E1876-15: Standard test method for dynamic Young's modulus, shear modulus, and Poisson's ratio by impulse excitation of vibration. American Society for Testing Materials International, West Conshohocken, USA. Available online at: https://www.astm.org/Standards/E1876.html. [Accessed: 30 July 2021]
11. Tognana S, Salgueiro W, Somoza A, and Marzocca A (2010). Measurement of the Young's modulus in particulate epoxy composites using the impulse excitation technique. *Materials Science and Engineering*: A, 527(18): 4619-4623.